Review

Fractality: An Adaptive Evolutionary Conserved Bioengineering Design of the Gas Exchangers

John Ndegwa Maina *

Posted Date: 15 December 2025

doi: 10.20944/preprints202512.1208.v1

Keywords: fractality; lung; chorioallantoic membrane; labyrinthine organs; trachea; pores; gills; biomimicry

 doi:10.20944/preprints202512.1208.v1

Review

Fractality: An Adaptive Evolutionary Conserved Bioengineering Design of the Gas Exchangers

John N. Maina

Department of Zoology, Auckland Park Campus, University of Johannesburg, Johannesburg 2006, South Africa; jmaina@uj.ac.za

Abstract

In biology, termed 'Bauplans' (body plans), 'ground plans' and 'blue-prints', fractality is a noteworthy evolutionary extensively conserved morphological feature. Particularly in the last six decades, fractal geometry (FG) has advanced from a mere intellectual concept to a branch of applied mathematics of considerable heuristic value and important practical application in as diverse fields as engineering, architecture, medicine and social sciences. FG meaningfully explicates morphological- and physiological states and processes. In medicine, it quantitatively characterizes abnormalities, pathologies and diseases. Here, we show that across animal taxa, structurally, gas exchangers are inherently fractal. Whilst providing optimal flow conditions of the respiratory fluid media (RFM) (air/water and blood), branching morphology optimizes respiratory surface area. For the lungs, tight patterning and proximation of the functional parts brings the RFM close, enhancing gas exchange by passive diffusion. Except for the lung, brain, blood vessels, kidney and nervous system, few organs and tissues have been morphologically analyzed to the extent of determining their fractal dimensions. Such detailed studies are urgently required. They should instructively inform on why and how diseases and pathologies affect some organs and tissues and not others. Furthermore, biomimetically, they may instruct on the most effective ways of designing efficacious artificial supporting devices.

Keywords: fractality; lung; chorioallantoic membrane; labyrinthine organs; trachea; pores; gills; biomimicry

1. Introduction

Optimal levels of chaos and fractality are distinctly associated with physiological health and function in natural systems. [1]

Fractality or self-similarity is an elemental structural property of many, if not all, complex physical- and natural assemblages [2–12]. Fractal geometry (FG) has been designated as the 'design of nature' [3,4,9–13]. The physicist, polymath and information theorist Benoit B. Mandelbrot (1924-2010), whose broad interest was in the inexactness and stochasticity of natural forms, phenomena and processes, conceived the word '*fractal*' from the Latin word '*fractus*', *meaning* 'fragmented', 'uneven' and 'broken' [2,3]. FG is a branch of applied mathematics which characterizes complicated states and phenomena. It has been meaningfully applied to analyze complex structures and processes in diverse disciplines such as architecture, physics, engineering, chemistry, physiology-, pathology, pathogenesis of diseases, morphogenetic development and even in aspects such as human language, information technology, cognitive development, consciousness, urban growth and the dynamics of capital markets [14–29]. Among other properties, fractal forms and mechanisms exhibit well-ordered iteration, space-filling, self-similarity and scale invariance [2,3]. To various extents and levels of organization, practically all biological assemblages exhibit fractality [4,30–35]. Mathematically, fractalities are holistically expressed by power law functions, where the fractal dimensions (D_F) are

 doi:10.20944/preprints202512.1208.v1

non-integer exponents [2–4,36–38]: inclusively, D_F denotes the structural complexity of a self-similar natural assemblage.

Respiration is the mechanism by which molecular O_2 is acquired and at cellular level (in the mitochondria) utilized to generate energy in form of ATP (adenosine phosphate) which drives the metabolic processes: CO_2, a byproduct of the process, is eliminated [39–41]. It comprises highly coordinated central neural control, a battery of sensory input systems, functionally efficient ventilatory mechanisms and well-developed and effective gas exchangers, i.e., respiratory organs [42–45]. Animals will generally live for weeks without food, days without water and only minutes without molecular O_2 [46]. From its important role in driving metabolic processes, Max Kleiber [47] termed molecular O_2 as 'the fire of life'. Adequate acquisition of O_2 was an evolutionary necessity to realization of the structural- and functional novelties which permitted animals to live and thrive under dynamically different environmental conditions and lead different lifestyles [43,48–53]. With trees being the most abundant and conspicuous examples, branched or dendritic structures preponderate in nature [54–59]. For the human lung, forming what is commonly termed 'respiratory tree', the branched bronchial (airway) morphology comprises a recursive assemblage of as many as twenty-three branches that terminate in a 'crown = canopy' of millions of the microscopic alveoli [38,60–62]. The regular branching of the bronchial- and the vascular systems (the pulmonary artery and vein) of the mammalian lung allow optimal flows of air and blood in the lung [32,63–69].

Here, the morphologies of various gas exchangers of phylogenetically diverse animal taxa are compared. It is shown that the principal structural components fundamentally share a branched structure. The design generates large respiratory surface area (RSA) in confined spaces while a close patterning and proximation of the passageways (airway- and the vascular systems) brings the respiratory fluid media, respectively air/water and blood, into close-proximity across thin tissue partitioning, a structural feature that enhances gas exchange by passive diffusion (60-62). In evolutionary terms, fractality is an important conserved structural design which importantly explains the layouts of the functional components of tissues, organs and organ systems.

2. Gas exchangers

In different animal taxa, developed to various levels of structural complexity and functional efficiency, alongside other roles, gas exchangers (respiratory organs) are foremost involved in respiration, i.e., acquisition of O_2 and elimination of CO_2. Mammals and birds, the primary vertebrates which have evolved full endothermic-homeothermy, possess exceptionally morphologically complex and physiologically efficient gas exchangers [61–63,70,71] with the main structural- and functional systems comprising the airway- and the vascular (pulmonary artery and vein) systems. Anatomically, the parts track and pattern each other and closely proximate (Figure 1a-d; e-h). A constellation of gas exchangers has evolved in the animal life [43].

 doi:10.20944/preprints202512.1208.v1

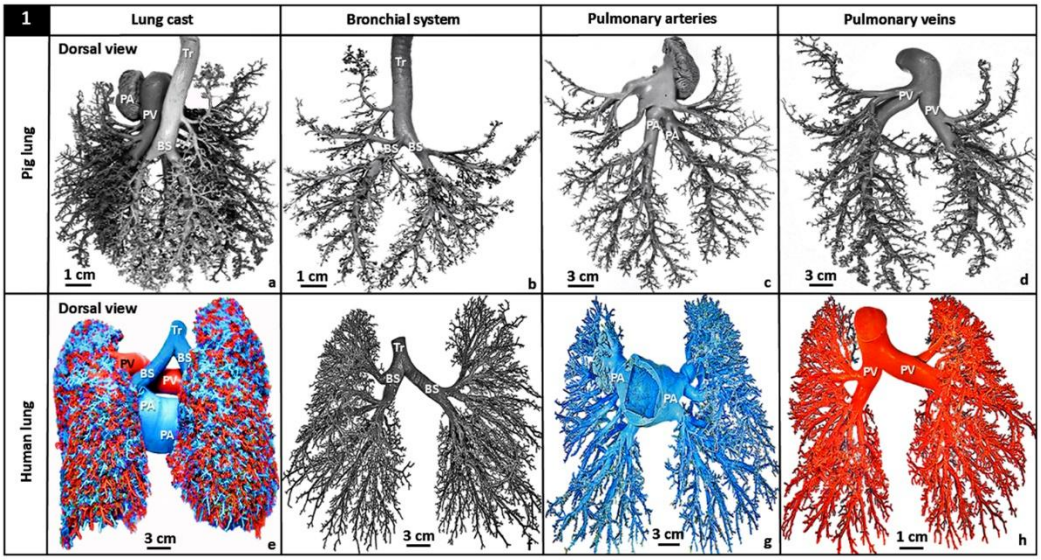

Figure 1. Triple latex rubber cast preparations of the pig- (*Sus scrofa*) **(a-d)** and the human (*Homo sapiens*) lungs **(e-h)**. The dorsal views of the casts of the main parts of the lungs, namely the airway (bronchial-) system (BS), the pulmonary artery (PA) and the pulmonary vein (PV). The lengths, the diameters and the angles of bifurcation of the individual parts were determined after physical separation of the parts of the cast (lung): **b-d** for the pig- and **f-h** for the human lung. They show the similarities of the branching pattern and the proximity of the airway- and the vascular parts of the lungs. Tr, trachea.

2.1. Bronchioalveolar (Mammalian) Lung

The volume of the mammalian, i.e., bronchioalveoar, lung is determined by that of the thoracic cavity (chest) which is bordered by the thoracic vertebrae (dorsally), ribs (laterally) and the diaphragm (caudally): extensive RSA and large pulmonary capillary blood volume (PCBV) are optimized in a limited space. For a 74 kg body mass person, while the mean total lung volume is ~4.3 L, the RSA is 143 m^2 and the PCBV is 213 cm^3 [72]. Although outstandingly large, as observed by Rao and Johncy [73], it is important to correct a statement which often appears especially in the popular literature and unfortunately in journal articles that the RSA of the human lung is equivalent to that of a tennis court. While the surface area of a tennis court, which most people are familiar with, is an informative example, the claim lacks scientific validity and it is a clear overstatement. The surface area of a double's tennis court is ~262m^2 while that of a single's one is 196m^2: the RSA of the human lung does not meet either of the measurements.

The vast RSA of the vertebrate lung is achieved by the regular branching of the bronchial- and the vascular systems (Figure 1). For the human lung, illustratively, Weibel [74] compared the compacting of the bronchial- and the vascular systems in the human lung to folding a piece of A-4 size paper to fit into a thimble! At regular intervals, the bronchial- and the vascular systems branch at constant angles and decrease in diameter at consistent ratios [38,60–62] (Figure 2), structural properties which optimize air- and blood flows, making ventilatory- and perfusive functions cost-effective [71,75–77]. The morphological patterning and tight packing of the airways- and the blood vessels of the vertebrate lungs [58,60–62] (Figure 1) develops by a widely conserved processes termed branching morphogenesis [10,32,38,78–83] which is well-regulated spatiotemporally expression of various molecular cues or growth factors [10,32,38,78–83].

 doi:10.20944/preprints202512.1208.v1

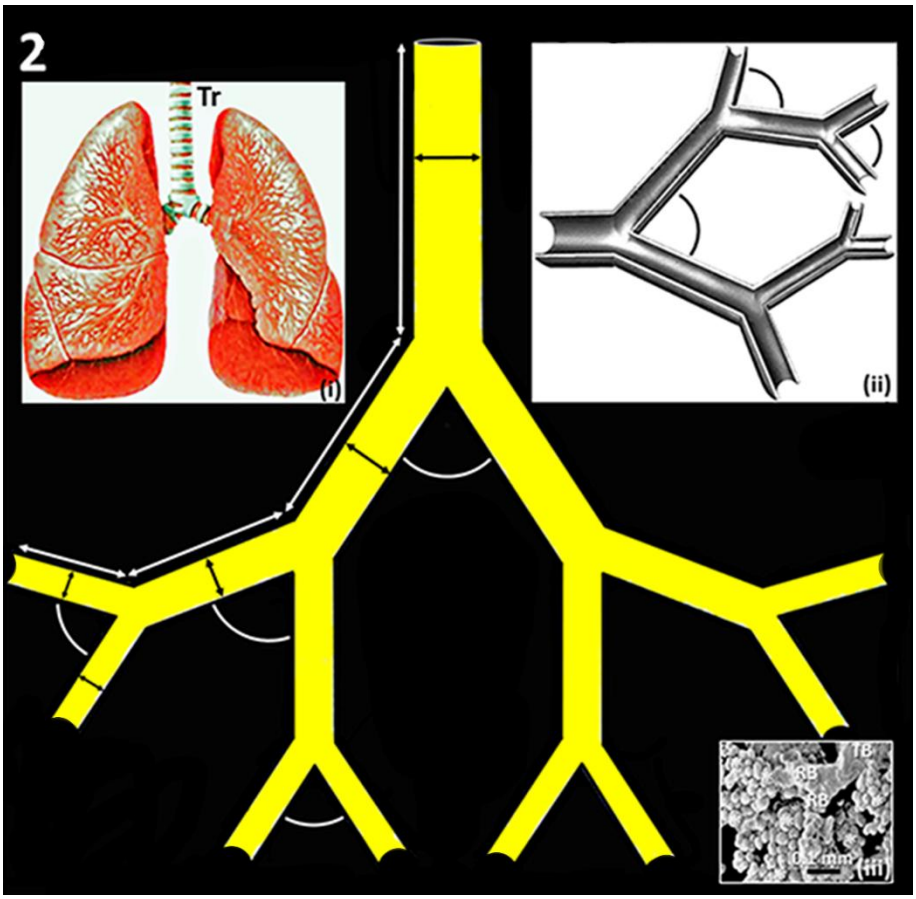

Figure 2. Dichotomous branching of the bronchial (airway) system of the vertebrate lung. The lengths of the conduits are shown by white double-sided arrows (↕), branching angles by arcs and diameters by black double-sided arrows (↕). **Inserts: (i)** – Illustration of the human lung showing trachea (Tr) which bifurcates into left- and right primary bronchi which branch into lobar bronchi and progressively into smaller airways to form the so-called 'respiratory tree'; **(ii)** – Diagram showing airways branching at regular intervals (arcs) and; **(iii)** – Scanning electron micrograph showing the terminal passageways of the airway system of the human lung. TB, terminal bronchus; RB, respiratory bronchioles; asterisks - ∗, alveoli.

The bronchial system of the human lung comprises 23 branches that terminate in ~500 million alveoli [60–62,84–88]. Originating from the right ventricle, the pulmonary artery of which compared to the pulmonary vein branches and patterns relatively more closely to that of the b**ronchial tree [62],** generates ~70 million precapillary arterioles, >250,000 arterioles and 280 billion blood capillary segments which contain ~200 cm^3 of pulmonary capillary blood volume [72,89]. After blood is oxygenated in the lung, it is returned to the heart via the pulmonary vein [90,91]. From their morphologies, Lefevre [75] determined that the blood vessels of the human lung are characteristically fractal. For the pulmonary vascular systems of the pig- (Figure 1a-d), the human- (Figure 1e-h), the dog- and the cat lungs, the angles of bifurcation are constant across the generations and the diameters decrease at about a constant ratio [61,92–98] (Figure 2). In the vertebrate lungs, the branching diameter value of the airways is about the perfect measure which accords with the Hess-Murray's Law of Hemodynamics [64]: the flow of air obeys what has been termed 'principle of minimum work' or 'principle of adequate design' [59,76,99].

The morphologies and morphometries of the bronchial- and the vascular systems of the pig- [98] (Figure 1 a-d) and the human lungs [38] (Fig. e-h) have been investigated by latex rubber cast preparations: the diameters and the lengths of the constitutive parts and their angles of bifurcation were determined. For the human lung, the diametric- and the length D_{Fs} of the three main structural components were determined by plotting the total branch diameters against the mean branch diameters and the total branch lengths against the mean branch lengths on double logarithmic

 doi:10.20944/preprints202512.1208.v1

graphic scales [38] (Figure 3). For the bronchial system, the pulmonary artery and the pulmonary vein, the diameter-based D_{Fs} were respectively 2.714, 2.882 and 2.334 while the respective length-based D_{Fs} were 3.098, 3.916 and 4.041 [38]. The relatively greater length-based D_{Fs} suggested that compared to diameters, branch lengths may contribute more to the fractality of the structures. The high D_{Fs} of the bronchial and the vascular systems of the structural components of the human lung show the high fractality, i.e., intense space-filling properties, of the three main structural parts of the organ (Figure 3).

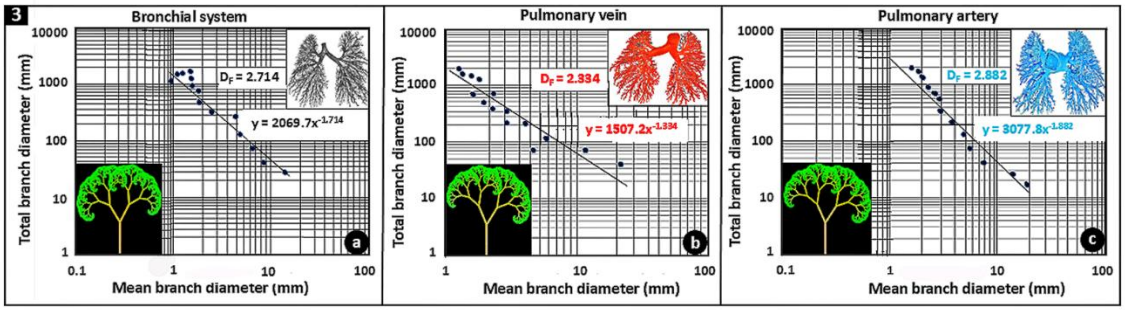

Figure 3. Double logarithmic plots of the total branch diameters against the mean branch diameters of the latex rubber cast preparations of the bronchial (airway) system **(a)**, the pulmonary vein **(b)** and the pulmonary artery **(c)** of human lung: respectively, the fractal dimensions (D_{Fs}) were 2.714, 2.334 and 2.882. **Inserts:** For each part of the lung, the top right figure is a separated preparation while bottom left one is a computer-generated reconstruction of the lengths and angles of bifurcation. The reconstructions were performed with an Open-access program found at 'http://mwskirpan.com/FractalTree/' (accessed 07-08-2020), courtesy of Michael Warren, Skirpan of Carnegie Mellon University.

2.2. Parabronchial (Avian) Lung

Among the air-breathing vertebrates, the avian respiratory system (the lung-air sac system) is structurally the most complicated and functionally the most efficient [43,100–106] (Figure 4a-f). The bronchial system of the parabronchial (avian) lung comprises a three-tiered hoop-like assemblage of bronchial passageways which comprise an intrapulmonary primary bronchus, four sets of secondary bronchi (SB) and many parabronchi (tertiary bronchi) which interconnect the SB [103,106] (Figure 4a-d). Like for the pig (*Sus scrofa*)- [98] (Figure 1a-d) and the human lungs [38] (Figure 1e-h), the bronchial- and the vascular systems of the avian lung closely track and pattern each other (Figure 4e). However, while the three main structural parts of the mammalian lung branch by regular dichotomy [85,86,89,94,107] [Figures 1; 2 (ii, iii)], the avian ones develop by monopodial branching [108,109] (Figure 4g-j). For the avian lung, the different developmental process may increase the number of hexagonal-shaped parabronchi which contain gas exchange tissue in relatively smaller lungs [43,48,49,100,101,103,104,106,110,111]. The structure of the circulatory system of the avian lungs has been well-investigated [112–118]. The pulmonary artery and vein, which respectively deliver deoxygenated (venous) blood to the lung (from the heart) and return oxygenated (arterial) blood to it, closely follow each other (Figures 4e). Although the D_{Fs} of the bronchial-, the pulmonary artery- and the pulmonary veins of the avian lung have not yet been determined, the particularly complex morphological organizations of the structures (Figure 4a-f) suggest high fractalities.

 doi:10.20944/preprints202512.1208.v1

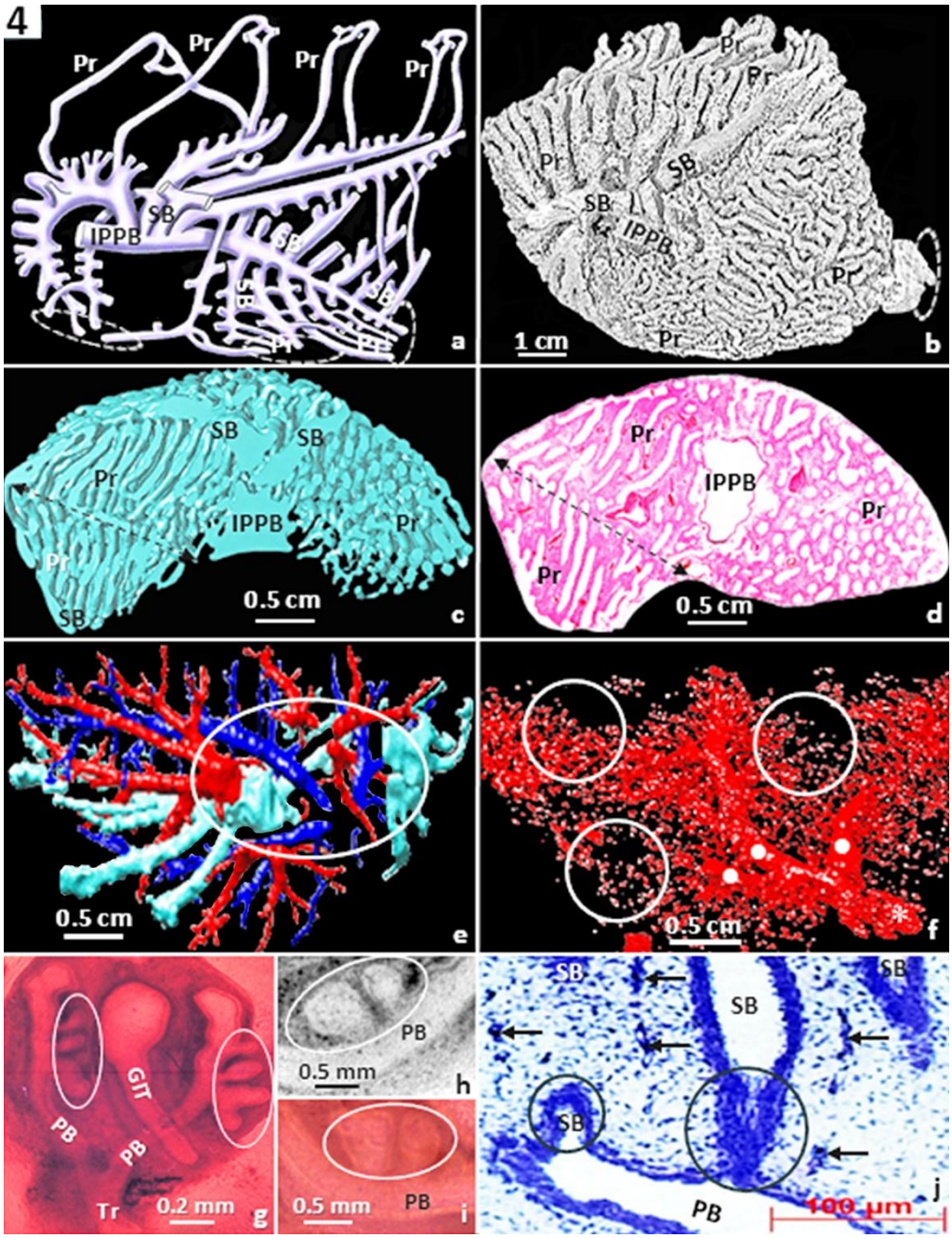

Figure 4. The complex airway (bronchial) morphology of the avian lung **(a)**. IPPB, intrapulmonary primary bronchus; SB, secondary bronchi; Pr, parabronchi; encircled (dashed) areas, ostia. Latex rubber cast preparation of the lung of the domestic fowl (*Gallus gallus* variant *domesticus*) (**b**) showing the complex and tightly packed airways. IPPB, intrapulmonary primary bronchus; SB, secondary bronchi; Pr, parabronchi; encircled (dashed) area, an ostium. Three-dimensional computer reconstruction **(c)** and histological preparation **(d)** of the lung of the domestic fowl showing the complex arrangements of the airways. IPPB, intrapulmonary primary bronchus; SB, secondary bronchi; Pr, parabronchi; double-sided (dashed) arrows, line of anastomosis, where the parabronchi, from the medioventral secondary bronchi connect and those from the mediodorsal secondary bronchi connect. Three-dimensional (3D) computer reconstruction of the bronchial- (cyan) system, the pulmonary vein (red) and the pulmonary artery (blue) of the lung of the domestic fowl **(e)**: the parts pattern and track each other closely. Encircled area, hilum. 3D computer reconstruction of an interparabronchial vein (asterisk - ∗) of the lung of the domestic fowl giving rise to intraparabronchial arteries (dots - •) (**f**). Circles (○), blood capillaries. Developing lung of the egg of the domestic fowl showing monopodial branching of the secondary bronchi (encircled areas, O) **(g-j)**. Tr, trachea; PB, primary bronchus; GIT, gastrointestinal tract; arrows (↑), developing blood vessels, which also display monopodial branching.

 doi:10.20944/preprints202512.1208.v1

2.3. Insectan Tracheal System

Among the gas exchangers that have evolved in multicellular animals, the tracheal system of insects is unique in that O_2 is delivered directly from air to the body tissues and cells at extremely high partial pressure of O_2 (PO_2) [119–122]. The respiratory mechanism profoundly varies from that which exists in 'lunged' animals, where a circulatory system separates the gas exchanger (respiratory organ) from the tissues and cells of the body, a point at which the PO_2 has decreased close to zero. Compared with the bronchial system of the vertebrate lungs, the insectan tracheal system delivers ten times more O_2 per gram body tissue [123]. The tracheal system, which saturates the insectan body, comprises a copious system of branched conduits (Figure 5a) which are strengthened by spiral coils of chitin that are called taenidia. Adaptively, the volume density of the tracheal system of an insect's body per unit body mass correlates with attributes such as body size, metabolic capacity and the PO_2 in the air [120–125]. As the trachea branch, they narrow and become thin-walled [120,121,126,127]. At the point they enter tissues, the passageways are termed tracheoles [Figure 5a (ii)]. In the extremely highly metabolically active insects such as dragon flies (Order: Odonata), for tissues such as the flight muscles, to reduce the diffusional distances of O_2, the tracheoles depress the cell walls to end very close to the mitochondria [121,123,128]. Like for the bronchial system of the mammalian- [60–62] (Figure 1) and the avian lungs [85,86,129] (Figure 4a-d), the tracheal system of insects develops by the conserved process of branching morphogenesis which is controlled by well-regulated spatiotemporal expression of growth (molecular) factors [38,129–131]. For the insectan tissues and cells, the branching and hence the fractality of the tracheal system provides efficient delivery of O_2 and elimination of CO_2.

 doi:10.20944/preprints202512.1208.v1

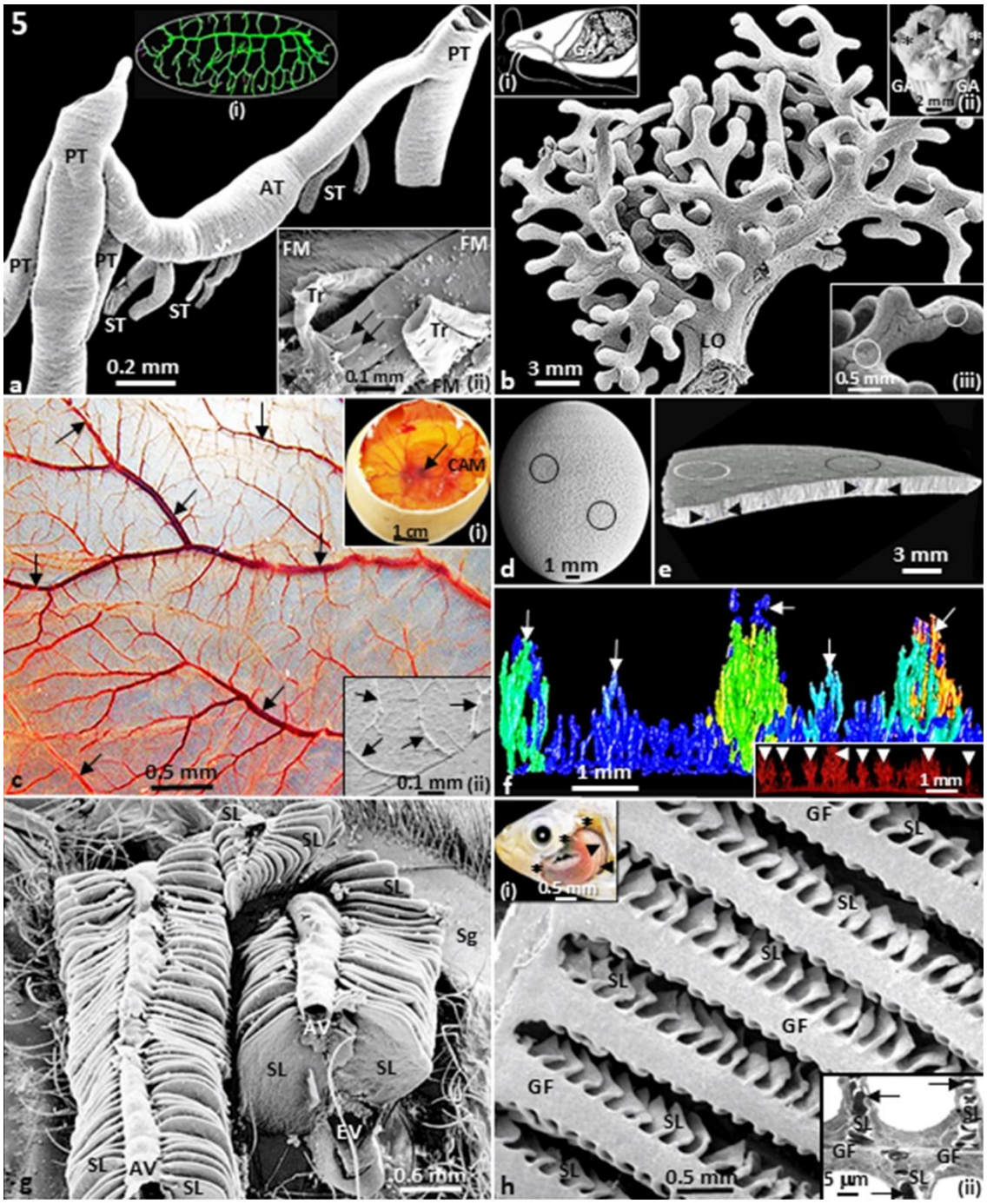

Figure 5. Insectan tracheal system of the grasshopper (*Chrotogonus senegalensis*) **(a)**. PT, primary trachea; ST, secondary trachea; AT, anastomosing trachea. **Inserts: (i)** – Copious tracheal system of a pupa of cecropia moth (*Hyalophora cecropia*); **(ii)** – Terminal trachea (Tr) and tracheoles (arrows) of the flight muscles (FM) of the grasshopper. The branched morphology of a labyrinthine organ (LO) of a catfish (*Clarias gariepinus*) **(b)**. **Inserts: (i)** – Diagram of the head region of a catfish (*C. gariepinus*) showing the location of the labyrinthine organs (asterisks, ∗). GA, gill arches; **(ii)** – Respiratory structures of the catfish (*C. gariepinus*) showing the suprabrachial membranes (arrow heads, ►), gill fans (dots, •), labyrinthine organs (asterisks, ∗) and gill arches (GA); **(iii)** – Close-up of the surface of a labyrinthine organ showing the intense vascularization of its surface (circles). Surface of the chorioallantoic membrane (CAM) of the egg of an ostrich (*Struthio camelus*) at day 26 of incubation **(c)**. The CAM is intensely vascularized by liberally branching blood vessels (arrows – ↓). **Inserts: (i)** – Egg of an ostrich opened on the air-cell end to show the well-vascularized CAM, with the developing embryo at the center (arrow, ↓); **(ii)** – Scanning electron micrograph showing the vascularization of the CAM (arrows - ↓). Ostrich egg showing pores which perforate the shell (circles, ○) **(d)**. Side view of a piece of the ostrich egg-shell showing pores from the surface aspect (encircled areas – O) and across the thickness of the shell (arrowheads – ►) **(e).** Microcomputer

 doi:10.20944/preprints202512.1208.v1

tomography (μCT) scan of the ostrich egg-shell showing the branched morphology of the pores (arrows) (**f**). **Insert:** Pores of the ostrich egg-shell which display 'tree-like' shape (arrow heads – ►). Gills of the crab (*Potamon niloticus*) showing the tight arrangement of the secondary lamellae (SL), where gas exchange occurs (**g**). AV, afferent blood vessels; EV, afferent blood vessels; Sg, scaphognathite, structures which ventilates the gills. Gill filaments (GF) of a gills (branchial) arch of a tilapiine fish (*Alcolapia grahami*) giving rise to numerous secondary lamellae (SL) **(h)**. **Inserts: (i)** – Gill arches (arrow heads – ►) which are covered by an operculum (asterisks – ∗), which is here removed to show the gill arches; **(ii)** – Transmission electron micrograph showing a gill filament (GF) giving rise to secondary lamellae (SL). Arrows (↓), erythrocytes.

2.4. Labyrinthine Organs of Catfishes

Depending on environmental conditions, bimodal-breathing or transitional fish such as the catfishes (Order: Siluriformes) adaptively acquire O_2 from both water (using gills) and air by means of so-called accessory respiratory organs (AROs) [132–139]. The AROs comprise the suprabranchial chamber membranes and the labyrinthine organs (LOs) [132–139] (Figure 5(ii). The LOs largely originate from the second- and fourth gill arches and slot into the suprabranchial chambers, concavities that are located dorsal to the brachial (gill) arches [Figure 5a (i)]. Termed 'dendritic or arborescent organs', morphologically, the LOs are 'tree-like' dichotomously branched structures (Figure 5b). Their surfaces are well-vascularized [Figure 5(iii)]. The fractality of the LOs optimizes the RSA in the limited space which is bordered by the hard-walled suprabranchial chambers.

2.5. Chorioallantoic Membrane of the Avian Egg

Regarding the cleidoic (self-supporting = self-containing) avian eggs, gas exchange occurs by diffusion across the pores which perforate the calcaneous shell and during incubation across the chorioallantoic membrane (CAM) to support embryonic development (Figure 5c). The CAM, which is a simple extraembryonic membrane (Figure 5c), also plays other important functions such as transfer of calcium from the shell to the embryo for growth and development especially of bones, maintaining acid-base homeostasis, ion- and water reabsorption from and storage of excretory waste products in the allantois [140–143]: from its respiratory- and nourishment roles, the CAM is analogous to the placenta of the viviparous mammals. The CAM develops by fusion of the splanchnic mesoderm of the allantois and the somatic mesoderm of the chorion [144]. To promote acquisition of O_2 during embryonic development, vascularization of the CAM increases significantly [145–148]: the process occurs by the morphogenetic process of branching morphogenesis which is regulated by well-regulated spatiotemporal expression of molecular (growth) factors [78,81,82,145,149]. The fractality of the CAM vasculature (Figure 5c) increases the RSA and blood volume, features which increase respiratory efficiency.

2.6. Pores of the Ostrich Egg-Shell

Among the extant species of birds, weighing as much as 2 kg, the ostrich (*Struthio camelus*) egg [Figure 5c(i); d] is the largest and the mean thickness of the shell (Figure 5e) is as sizable as 2 mm [147,150]. Together with physically protecting the developing embryo and regulating water loss, the egg-shell performs an important respiratory function. Oxygen and CO_2 diffuse across the pores (Figure 5d, e) which are more plentiful on the blunt end on the shell, i.e., the air-cell part [147,150]. In various parts of the shell, the shapes and sizes of the pores remarkably vary in size and morphology [150] (Figure 5f). Generally, they display complex tree-like, i.e., branched, (fractal) morphology (Figure 5f) should promotes transfer of respiratory gases across a thick shell.

2.7. External Gills

Gills are evaginated respiratory outgrowths which are permeable to respiratory gases, i.e., O_2 and CO_2 (Figure 5g; h): well-perfused with blood and ventilated with water, they evolved for water-breathing. From their location and morphology, gills are categorized as either external- or internal types [151]: the former, which are structurally less elaborate and functionally less efficient, dangle

 doi:10.20944/preprints202512.1208.v1

freely into surrounding water while the later, which are more derived and structurally- and functionally more efficient are either covered by a mesenchymal tissue mass (e.g., for elasmobranchs, i.e., sharks) or a movable operculum (e.g. in teleosts) [Figure 5h(i)]. For the teleosts, the gills commonly comprise four pairs of gill arches that are contained in the branchial cavity [Figure 5h(i)].

Teleost gills comprise hundreds of gill filaments that branch into thousands of thin flap-like semicircular-shaped secondary lamellae [151–156] [Figure 5g, h]. Gas exchange occurs across the very thin water-blood barriers of the secondary lamellae [Figure 5h(ii)]. The hierarchical, i.e., stratified or branched, morphology of the teleost gills presents a fractal design which generates large respiratory surface area in a limited space, i.e., the brachial cavity. Compared to more sluggish species, more active fish species such as the streamlined tuna have relatively greater total gill respiratory surface areas which are achieved from greater numbers and closer spacing of secondary lamellae [151].

3. Conclusions

During the evolution of life, a process that has spanned a period of ~4 billion years [157,158], nature has tinkered with, crafted and optimized a collection of functional contrivances (traits) to overcome existing adversities. By exploiting such 'solutions', biomimetic studies have expedited engineering of solutions to challenges which humans face [159–162], [https://www.linkedin.com/pulse/biomimicry-engineering-design-learning-uohae, accessed on 18-11-2925]. Compared to the conventional 'trial-and-error' practice in engineering, mimicking nature (biomimicry) very so often presents more efficient and cost-effective resolutions to technology-centered problems, especially those regarding resource and energy utilization efficiency and resilience [163,164]. Fractal geometry explains how at various scales of organization, self-similar, i.e., iterated, properties generate profoundly robust and efficient biological assemblages. West [165] observed that 'the fractal concept provides a mechanism for the morphogenesis of complex structures which are more stable than those generated by classical scaling, i.e., they are more error tolerant'. In biology, incontrovertibly, fractality is an adaptive novelty [7,10,27,32] which confers optimal utilization of spaces, which in animal bodies are always at premium [68]. For gas exchangers, branched or well-ordered morphology increases the RSA, a structural feature which increases passive diffusion of O_2 and CO_2 between respiratory fluid media. For the brain, copious neuronal networks specify efficient communication. Many other structural components of the animal body, e.g., the airway and the vascular systems, display complex fractal properties which cannot be meaningfully quantified by the traditional Euclidean geometry. In medicine, the non-integer fractal dimension (D_F) or scaling exponent is a highly instructive diagnostic tool [166–170]. Alteration from normal structure to abnormal, pathological- and disease states consequences in measurable change in fractality [25,166–170]: healthy organs/structures appear to have D_{Fs} which fall within a narrow range while disease and pathological conditions consequence in alteration of the normal fractality. Determination of D_{FS} from medical images such as those acquired by magnetic resonance imaging (MRI), microComputer tomography (μCT), X-ray and histological tissue preparations or time-series signals such as electroencephalogram (EEG), magnetoencephalography (MEG) and electrocardiogram (ECG) now provide physicians with resources on which after application of, e.g., fractal analysis various diseases and conditions can be diagnosed often much earlier than it is possible by traditional clinical methods [169,171–177]. Recently, application of FG was recognized as one of the important medical advances of non-invasively diagnosing diabetic retinopathy [170]. For the bronchial tree of the human lung, decrease of the D_F, which presents as decrease in branching complexity, ensues from respiratory diseases such as chronic obstructive pulmonary disease (COPD) [168] and for the brain, decrease of the D_F of the neural network is associated with Alzheimer's disease [23,178–180]. Furthermore, application of FG provides a new method of evaluating physiological states such as cardiac risk and assessment of the aging process [20,173,177]. Although in the recent past noteworthy progress has been made in application of FG towards understanding the functional designs of biological states and processes, only very few organs have been thoroughly and comprehensively analyzed to the degree of determining the D_{Fs}. Differences of the fractalities of the structural

 doi:10.20944/preprints202512.1208.v1

components of the various organs and tissues of different animal species may explain the variations of the predispositions of tissues and organs to pathogens, diseases and pathological afflictions. Moreover, the data may be instructive in the formulation of effective human interventions.

Funding The preparation of this paper was supported by the National Research Foundation of South Africa (NRF). I am most grateful for their funding my research engagements.

Data Availability All data are available in this article.

Conflicts of Interest There are no conflicts of interest to declare.

Ethics Approval Not applicable.

Artificial Intelligence (AI) The author declares that AI-generated work has not been used in this work.

References

1. Korolj A, Wu HT, Radisic M. A healthy dose of chaos: using fractal frameworks for engineering higher-fidelity biomedical systems. Biomaterials 2019; 219:119363.
2. Mandelbrot B. How long is the coast of Britain? Statistical self-similarity and fractional dimension. Science 1967; 156:636–638.
3. Mandelbrot B. Form, chance, and dimension. New York, Freeman; 1977.
4. Mandelbrot B. The fractal geometry of nature. New York, Freeman; 1983.
5. Eshel A. On the fractal dimensions of a root system. Plant, Cell Environm. 1998; 21:247–251.
6. Brown JH et al. The fractal nature of nature: power laws, ecological complexity and biodiversity.Philos. Trans. R. Soc. Lond., B, Biol. Sci. 2002; 357:619–626.
7. Weibel E. Mandelbrot's fractals and the geometry of life: a tribute to Benoit Mandelbrot on his 80th birthday. Fractals Biol. Med. 2005; 4:1–14.
8. Losa GA. The living realm depicted by the fractal geometry. Fractal Geometry and Nonlinear Anal in Med. and Biol. 2015; 1:11–15.
9. Mandelbrot B. Is nature fractal? Science 1998; 279:783–784.
10. Weibel ER. Design of biological organisms and fractal geometry. In: Nonnenmacher TF, Losa GA, Weibel ER, Editors. Fractals in biology and medicine, mathematics and biosciences in interaction. Basel, Birkhäuser, 1993. pp. 1–2.
11. Ball P. The self-made tapestry: pattern formation in nature. Tequests (FL): The Booksellers; 2001.
12. Ball P. Patterns in nature: why the natural world looks the way it does. Chicago (IL): University of Chicago Press; 2016.
13. Göran P, Nachtigall W. Biomimetics for architecture and design: nature – analogies – technology. Switzerland: Springer (Cham); 2015.
14. Bassingthwaighte JB. Fractal vascular growth patterns. Acta Stereol. 1992;11:305–319.
15. Bassingthwaighte JB, Liebovitch LS, West BJ. Fractal physiology. Oxford: Oxford University Press; 1994.
16. West BJ. Deering W. Fractal physiology for physicists: Lévy statistics. Physics Reports 1994; 246:1–100.
17. Peters E. Chaos and order in the capital markets: a new view of cycles, prices, and market volatility. New York: Wiley; 1996.
18. Altemeier WA, McKinney S, Glenny T.W. Fractal nature of regional ventilation distribution. J. Appl. Physiol. 2000; 88:1551–1557.
19. Oczeretko E, Juczewska M., Kasacka J. Fractal geometric analysis of lung cancer angiogenic patterns. Folia Histochem. Cytobiol. 2001; 39:75–76.
20. Goldberger AL et al. Fractal dynamics in physiology: alterations with disease and aging. Proc. Natl Acad. Sci. (USA) 2002; 99:2466–2472.
21. Vlad MO et al. Functional, fractal nonlinear response with application to rate processes with memory, allometry, and population genetics. Proc. Natl. Acad. Sci. (USA) 2007; 104:4798–4803.
22. Delsanto PP et al. multilevel approach to cancer growth modelling. J. Theor. Biol. 2008; 250:16–24.
23. King RD et al. The Alzheimer's disease neuroimaging initiative: characterization of atrophic changes in the cerebral cortex using fractal dimensional analysis. Brain Imaging Behav. 2009;3:154–166.

 doi:10.20944/preprints202512.1208.v1

24. Popescu DP et al. Signal attenuation and box-counting fractal analysis of optical coherence tomography images of arterial tissue. Biomed. Optics Express 2010; 1:268–277.
25. Bizzarri M et al. Fractal analysis in a systems biology approach to cancer. Sem. Cancer Biol. 2011; 3:175–182.
26. Yanguang, C. Modeling fractal structure of city-size distributions using correlation functions. PLoS One 2011; 6:e24791.
27. Zdenek CC. The fractal nature of human consciousness, the evolution of the 'global human' and the driving forces of history. J. Conscious Evol. 2018; 4(4).https://digitalcommons.ciis.edu/cejournal/vol4/iss4/4
28. Vrdoljak A, Miletić K. Principles of fractal geometry and applications in architecture and civil engineering. *e-zb., Elektron. zb. rad*. 2019; 17:40–51.
29. Pethick J, Winter SL, Burnley M. Did you know? Using entropy and fractal geometry to quantify fluctuations in physiological outputs. Acta Physiologica 2021; 233:e13670.
30. Smith TG et al. A fractal analysis of cell images. J. Neurosci. Meth. 1989; 27:173–180.
31. Goldberger AL, West BJ. Fractals in physiology and medicine. Yale J. Biol. Med. 1987; 60:421–435.
32. Weibel ER. Fractal geometry: a design principle for living organisms. Am. J. Physiol. 1991; 261: L361–L369.
33. Losa GA, Nonnenmacher TF. Self-similarity and fractal irregularity in pathologic tissues. Mod. Pathol. 1996; 9:174–182.
34. Captur G et al. The fractal heart – embracing mathematics in the cardiology clinic. Nat. Rev. Cardiol. 2017; 14:56–64.
35. Shah RG et al. Fractal dimensions and branching characteristics of placental chorionic surface arteries. Placenta 2018; 70:4–6.
36. Vicsek T. Fractal growth phenomena. 2nd Ed. Singapore: World Scientific Book; 1992.
37. Falconer K. Fractal geometry: mathematical foundations and applications. New York: John Wiley and Sons Ltd.; 2003.
38. Essay M, Maina JN. Fractal analysis of concurrently prepared latex rubber casts of the bronchial and vascular systems of the human lung. Open Biol. 2020; 10:190249.
39. Napolitano G, Fasciolo G, Venditti P. The ambiguous aspects of oxygen. Oxygen 2022; 2:382–409.
40. Skulachev V et al. Six functions of respiration: Isn't it time to take control over ROS production in mitochondria, and aging along with it? Int. J. Mol. Sci. 2023; 24:12540.
41. Martín-Rodríguez AJ. Respiration-induced biofilm formation as a driver for bacterial niche colonization. Trends in Microbiol. 2023; 31:120–134.
42. Myers RM. What is respiration? School Sci. Math. 1946; 46:691–792.
43. Maina JN. The gas exchangers: structure, function, and evolution of the respiratory processes.Heidelberg: Springer-Verlag; 1998.
44. Perry SF, Burggren WW. Why respiratory biology? The meaning and significance of respiration and its integrative study. Integr. Comp. Biol. 2007; 47:506–509.
45. Webster LR, Karan S. The physiology and maintenance of respiration: a narrative review. Pain Ther. 2020; 9:467–486.
46. Danovaro R et al. The first metazoa living in permanently anoxic conditions. BMC Biology 2010; 8:30.
47. Kleiber M. The fire of life. New York: Wiley; 1961.
48. Maina JN. Comparative respiratory morphology: themes and principles in the design and construction of the gas exchangers. Anat. Rec. 2000; 261:25-44.
49. Maina JN. Fundamental structural aspects and features in the bioengineering of the gas exchangers: comparative perspectives. Adv. Anat. Embryol. Cell Biol. 2002; 163:1–108.
50. Jürgens KD, Gros G. Phylogenese der Gasaustauschsysteme [Phylogeny of gas exchange systems]. Anasthesiol. Intensivmed. Notfallmed. Schmerzther. 2002; 37:185–198.
51. Brown JH. Toward a metabolic theory of ecology. Ecology 2004; 85:1771–1789.
52. Glazier DS. Metabolic scaling in complex living systems. Systems 2014; 2:451–540.
53. Wilson DF, Matschinsky FM. Metabolic homeostasis in life as we know it: its origin and thermodynamic basis. Front. Physiol. 12:658997, 2021.

 doi:10.20944/preprints202512.1208.v1

54. Wilson TA. Design of the bronchial tree. Nature Lond. 1967; 213:668–669.
55. MacDonald N. Trees and networks in biological models. New York: John Wiley & Sons; 1983.
56. Mainster MA. The fractal properties of retinal vessels: embryological and clinical implicationsEye 1990; 4:235–241.
57. Turcotte DL, Pelletier JD, Newman WI. Networks with side branching in biology. J. Theor. Biol. 1998; 193:577–592.
58. Glenny, R.W. Emergence of matched airway and vascular trees from fractal rules. J. Appl. Physiol. 2011; 110:1119–1129.
59. Miguel AM. Dendritic design as an archetype for growth patterns in nature: fractal and constructal views. Front. Phys. 2014; 2:9.
60. Weibel ER, Gomez DM. Architecture of the human lung. Science 1962; 137: 577–585.
61. Weibel ER. Morphometry of the human lung. New York: Academic Press; 1963.
62. Weibel ER. The pathways for oxygen: structure and function in the mammalian respiratory system. Cambridge (MA): Harvard University Press; 1984.
63. Losa GA. The fractal geometry of life. Riv. Biol. 2009; 102:29-59.
64. Murray CD. The physiological principle of minimum work applied to the angle of branching of arteries. J. Gen. Physiol. 1926; 9:835–841.
65. Uylings HB. Optimization of diameters and bifurcation angles in lung and vascular tree structures. Bull. Math. Biol. 1977; 39:509–520.
66. Kassab GS. Scaling laws of vascular trees: of form and function. Am. J. Physiol. Heart Circ. Physiol. 2006; 290:H894–H903.
67. Stephenson D et al. Generalizing Murray's law: an optimization principle for fluidic networks of arbitrary shape and scale. *J. Appl. Phys.* 2015; 118:174302.
68. Hughes AD. Optimality, cost minimization and the design of arterial networks. Artery Res. 2015; 10:1–10.
69. Stephenson D, Lockerby DA. A generalized optimization principle for asymmetric branching in fluidic networks. Proc. R. Soc. A 2016; 472:20160451.
70. Kamiya A, Takahashi T. Quantitative assessments of morphological and functional properties of biological trees based on their fractal nature. J. Appl. Physiol. 2007; 102:2315–2323.
71. West JB. Respiratory physiology: the essentials. Philadelphia (PA): Lippincott Williams & Wilkins; 2012.
72. Gehr P, Bachofen M, Weibel ER. The normal human lung: ultrastructure and morphometric estimation of diffusion capacity. Respir. Physiol. 1978; 32:121–140.
73. Rao AA, Johncy S. Tennis courts in the human body: A review of the misleading metaphor in medical literature. Cureus 2022; 14:e21474.
74. Weibel ER. What makes a good lung? Swiss Med. Wkly. 2009; 139:375–386.
75. Lefevre J. Teleonomical optimization of a fractal model of the pulmonary arterial bed. J. Theor. Biol. 1983; 102:225–248.
76. Miguel AF. A general model for optimal branching of fluidic networks. *Physica A Stat. Mech. Appl*. 2018; 512:665–674.
77. Hopkins SR. Ventilation/perfusion relationships and gas exchange: measurement approaches. Compr. Physiol. 2020; 10:1155–1205.
78. Powers KA, Dhamoon AS. Physiology, pulmonary ventilation and perfusion. In: StatPearls [Internet]. Treasure Island (FL): StatPearls Publishing; 2024. https://www.ncbi.nlm.nih.gov/books/NBK539907/
79. Metzger RJ, Krasnow MA. Genetic control of branching morphogenesis. Science 1999; 284:1635–1639.
80. Warburton D. Developmental biology: order in the lung. Nature 2008; 453:733–735.
81. Warburton D et al. Growth factor signaling in lung morphogenetic centers automaticity, stereotypy and symmetry. Respir. Res. 2003; 19:294-315.
82. Metzger RJ et al. The branching programme of mouse lung development. Nature 2008; 453:745–750.
83. Hannezo E, Simons BD. Multiscale dynamics of branching morphogenesis. Curr. Opin. Cell Biol. 2019; 60:99–105.
84. Burri PH. Lung development and pulmonary angiogenesis. In: Gaultier CJ, Post M, editors. Lung disease. New York: Oxford University Press; 1999. pp. 122–151.

 doi:10.20944/preprints202512.1208.v1

85. Ochs M et al. The number of alveoli in the human lung. Am. J. Respir. Crit. Care Med. 2004; 169, 120 –124.
86. Schittny JC, Burri PH. Development and growth of the lung. In: Fishman AP, Elias JA, Fishman JA, Grippi MA, Kaiser, Senior RM, editors. Fishman's pulmonary diseases and disorders. New-York: McGraw-Hill; 2008. pp. 91–114.
87. Schittny JC. Development of the lung. Cell Tissue Res. 2017; 367:427–444.
88. Pan H, Deutsch GH, Wert SE. Comprehensive anatomic ontologies for lung development: a comparison of alveolar formation and maturation within mouse and human lung. J. Biomed. Semantics 2019; 10:18.
89. Horsfield TK. Morphometry of the small pulmonary arteries in man. Circ. Res. 1978;42:593–597.
90. Horsfield K, Gordon WI. Morphometry of pulmonary veins in man. Lung 1981; 159:211-218.
91. Horsfield, K. Functional morphology of the pulmonary vasculature. In: Chang HK, Paiva MŽ, editors. Respiratory physiology: an analytical approach. New York: Marcel Dekker Inc.; 1989. pp. 499–531, 1989.
92. Singhal S et al. Morphometry of the human pulmonary arterial tree. Circ. Res. 1973; 33:190–197.
93. Huang W et al. Morphometry of the human pulmonary vasculature. J. Appl. Physiol. 1996; 81:2123–2133.
94. Horsfield K, Cumming G. Morphology of the bronchial tree in man. J. Appl. Physiol. 1968; 24: 373–383.
95. Horsfield K, Relea FG, Cumming G. Diameter, length and branching ratios in the bronchial tree. Respir. Physiol. 1976; 26:351–356.
96. Thurlbeck A, Horsfield K. Branching angles in the bronchial tree related to order of branching. Respir. Physiol. 1980; 41:173–181.
97. Krenz GS, Linehan JH, Dawson CA. A fractal continuum model of the pulmonary arterial tree. J. Appl. Physiol. 1992; 72:2225–2237.
98. Maina JN, van Gils P. Morphometric characterization of the airway and vascular systems of the lung of the domestic pig, Sus scrofa: comparison of the airway, arterial and venous systems. Comp. Biochem. Physiol. A Mol. Integr. Physiol. 2001; 1130:781–798.
99. Rashevsky N. Mathematical biophysics: physico-mathematical foundations of biology. New York: Dover; 1960.
100. King AS. Structural and functional aspects of the avian lung and its air sacs. Intern. Rev. Gen. Exp. Zool. 1966; 2:171–267.
101. Duncker HR. The lung-air sac system of birds. A contribution to the functional anatomy of the respiratory apparatus. Ergeb. Anat. Entwicklung 1971; 45:1–171.
102. Scheid P. Mechanisms of gas exchange in bird lungs. Rev. Physiol. Biochem. Pharmacol. 1979; 86:137–186, 1979.
103. McLelland J. Anatomy of the lungs and air sacs. In: King AS. McLelland J, editors. Form and function in birds, vol. IV. London: Academic Press; 1989. pp. 221–279.
104. Maina JN. The lung-air sac system of birds: development, structure, and function. Berlin: Springer-Verlag; 2025.
105. Powell FL. Respiration. In: Scanes CG, editor. Sturkie's avian physiology, 6th edition. San Diego: Academic Press; 2014. pp. 301–336.
106. King AS, McLelland J. Birds: their structure and function, 2nd edition. London: Bailliéle Tindall; 1984.
107. Horsfield K. Diameters, generations, and orders of branches in the bronchial tree. J. Appl. Physiol. 1985; 68:457–461.
108. Maina JN. A systematic study of the development of the airway (bronchial) system of the avian lung from days 3 to 26 of embryogenesis: a transmission electron microscopic study on the domestic fowl, Gallus gallus variant domesticus. Tissue Cell 2003: 35:375–391.
109. Maina JN. Developmental dynamics of the bronchial (airway)- and air sac systems of the avian respiratory system from days 3 to 26 of life: A scanning electron microscopic study of the domestic fowl, Gallus gallus variant domesticus. Anat. Embryol. 2003; 207:119–134.
110. Maina JN. The morphometry of the avian lung. In: King AS, McLelland J, editors. Form and function in birds, vol.4. London: Academic Press; 1989. pp. 307–368.
111. Maina JN, King AS, Settle G. An allometric study of the pulmonary morphometric parameters in birds, with mammalian comparison. Philos. Trans. R. Soc. Lond. 1989; 326B:1–57.

 doi:10.20944/preprints202512.1208.v1

112. West NH, Bamford OS, Jones DR. A scanning electron microscope study of the microvasculature of the avian lung. Cell Tissue Res. 1977; 176:553–564.
113. Maina JN. Scanning electron microscopic study of the spatial organization of the air- and bloodconducting components of the avian lung (Gallus gallus domesticus). Anat. Rec. 1988; 222:145–153.
114. Abdalla MA. The blood supply to the lung. In: King AS, McLelland J, editors. Form and function in birds, vol. 4. London: Academic Press; 1989. pp. 281–306.
115. Woodward JD, Maina JN. A 3D digital reconstruction of the components of the gas exchange tissue of the lung of the muscovy duck, Cairina moschata. J. Anat. 2005; 206:477–492.
116. Woodward JD, Maina JN. Study of the structure of the air and blood capillaries of the gas exchange tissue of the avian lung by serial section three-dimensional reconstruction. J. Microsc. 2008; 230:84–93.
117. Maina JN, Woodward JD. Three-dimensional serial section computer reconstruction of the arrangement of the structural components of the parabronchus of the ostrich, Struthio camelus. Anat. Rec. 2009; 292:1685–1698.
118. Maina JN et al. 3D Computer reconstruction of the airway and the vascular systems of the lung of the domestic fowl, Gallus gallus variant domesticus. J. Appl. Math. Comput. 2021; 5:89–104.
119. Thorpe WH, Crisp DJ. Studies on plastron respiration. II. The respiratory efficiency of the plastron in Amphelocheirus. J. Exp. Biol. 1941; 24:270–303.
120. Wigglesworth VB. Insect physiology, 7th edition. London: Chapman and Hall; 1984.
121. Wigglesworth VB, Lee WM. The supply of oxygen to the flight muscles of insects: a theory of tracheole physiology. Tissue Cell 1982; 14:501–518.
122. Harrison JF. Tracheal system. In: Resh VH, Cardé RT, editors. Encyclopedia of insects, 2nd Edition. San Diego: Academic Press; 2009. pp. 1011–1015.
123. Steen JB. Comparative physiology of respiratory mechanisms. London: Academic Press; 1971.
124. Edwards GA, Ruska H, Harven de E. The fine structure of insect tracheoblasts, tracheae and tracheoles. Arch. Biol. 1958; 69:351–369.
125. Centanin L, Gorr TA, Wappner P. Tracheal remodelling in response to hypoxia. J. Insect Physiol. 2010; 56:447–454.
126. Scheid P, Hook C. Bridges CR. Diffusion in gas exchange of insects. Fed. Proc. Fed. Am. Soc. Expl. Biol. 1982; 30:1032–1034.
127. Snyder GK. et al. Gas exchange in the insect tracheal system. J. Theor. Biol. 1995; 172:199–207.
128. Maina JN. A scanning and transmission electron microscopic study of the tracheal air-sac system in a grasshopper (Chrotogonus senegalensis, Kraus)- (Orthoptera: Acrididae: Pygomorphinae). Anat. Rec. 1989; 223:393–405.
129. Maina JN. Comparative molecular developmental aspects of the mammalian- and the avian lungs, and the insectan tracheal system by branching morphogenesis: recent advances and future directions. Front. Zool. 2012; 9:16.
130. Samakovlis C. et al. Development of the Drosophila tracheal system occurs by a series of morphologically distinct but genetically coupled branching events. Development 1996; 122:1395–1407.
131. Affolter M, Caussinus E. Tracheal branching morphogenesis in Drosophila: new insights into cell behaviour and organ architecture. Development 2008; 135:2055–2064.
132. Graham JB. Air breathing fishes: evolution, diversity and adaptation. San Diego: Academic Press; 1997.
133. Maina JN, Maloiy GMO. The morphology of the respiratory organs of the African air-breathing catfish (Clarias mossambicus): a light, and electron microscopic study, with morphometric observations. J. Zool. Lond. 1986; 209:421–445.
134. Mbanga B, van Dyk C. Maina JN. Morphometric and morphological study of therespiratory organs of the bimodally-breathing African sharptooth catfish (Clarias gariepinus): Burchell (1822). Zoology 2018; 130: 6–18.
135. Maina JN. Functional morphology of the respiratory organs of the air-breathing fish with particular emphasis on the African catfishes, Clarias mossambicus and C. gariepinus. Acta Histochem. 2018; 120:613–622.

 doi:10.20944/preprints202512.1208.v1

136. Munshi JSD, Hughes GM. Air breathing fishes of india: their structure, function and life history. Rotterdam: AA Balkema Uitgevers; 1992.
137. Dehadrai PV, Tripathi SD. Environment and ecology of freshwater air-breathing teleosts. In: Hughes GM, editor. Respiration of amphibious vertebrates. London: Academic Press; 39–72, 1976.
138. Hughes GM, Munshi J.S.D. Fine structure of the respiratoty surfaces of an air-breathing fish, the climbing perch, Anabas testudineus (Bloch). Nature, Lond. 1968; 219:1382–1384.
139. Hughes GM, Singh BN. Respiration in air-breathing fish, the climbing perch, Anabas testudineus II. Respiratory patterns and the control of breathing. J. Exp. BioI. 1970; 53:281–298.
140. Coleman JR, Terepka AR. Fine structural changes associated with the onset of calcium, sodium and water transport by the chick chorioallantoic membrane. J. Membr. Biol. 1972; 7: 111–217.
141. Maksimov VF, Korostyshevskaya IM, Kurganov SA. Functional morphology of chorioallantoic vascular network in chicken. Bull. Exp. Biol. Med. 2006; 142:367–371.
142. Chien YC, Hincke MT, McKee MD. Ultrastructure of avian egg-shell during resorption following egg fertilization. J. Struct. Biol. 2009; 168:527–538.
143. Gabrielli MG, Accili D. The chick chorioallantoic membrane: a model of molecular, structural, and functional adaptation to transepithelial ion transport and barrier function during embryonic development. J. Biomed. Biotechnol. 2010; 2010:940741, 2010.
144. Romanoff AL. The extraembryonic membranes. In: Romanoff AL, editors. The avian embryo: structural and functional development. New York: The Macmillan Company. 1960. pp. 1039–140, 1960.
145. Makanya AN. et al. Dynamics of the developing chick chorioallantoic membrane assessed by stereology, allometry, immunohistochemistry and molecular analysis. PLoS One 2012; 11:e0152821.
146. Makanya AN, Jimoh SA, Maina JN. Methods of in ovo and ex ovo ostrich embryo culture with observations on the development and maturation of the chorioallantoic membrane. Microsc. Microanalysis 2023; 29:1523–1530.
147. Willoughby B. Morphological and morphometric study of the ostrich egg-shell with observations on the chorioallantoic membrane: a μct-, scanning electron microscope, and histological study. B.Sc. Honours Dissertation, University of Johannesburg; 2015.
148. Maina JN. Structure and function of the shell and the chorioallantoic membrane of the avian egg: embryonic respiration. In: Maina JN editor. The biology of the avian respiratory system.Cham (Switzerland): Springer; 2017. pp. 219–247.
149. Makanya AN. et al. Microvascular endowment in the developing chicken embryo lung. Am. J. Physiol. Lung Cell Mol. Physiol. 2007; 292:L1136–46.
150. Willoughby B et al. Micro-focus X-ray tomography study of the microstructure and morphometry of the egg-shell of ostriches (Struthio camerus). Anat. Rec. 2016; 299:1015–1026.
151. Hughes GM, Morgan M. The structure of the gills in relation to their respiratory function. Biol. Rev. 1973; 48:419–475.
152. Laurent P. Morphology and physiology of organs of aquatic respiration in vertebrates: the gill. J. Physiol. 1984; 79:98 –112.
153. Maina JN. A study of the morphology of the gills of an extreme alkalinity and hyperosmotic adapted teleost Oreochromis alcalicus grahami (Boulenger) with particular emphasis on the ultrastructure of the chloride cells and their modifications with water dilution. Anat. Embryol. 1990; 181:83–98.
154. Wilson JM, Laurent P. Fish gill morphology: inside out. J. Exp. Zool. 2002; 293:192–213.
155. Evans DH, Piermarini PM, Choe KP. The multifunctional fish gill: dominant site of gas exchange, osmoregulation, acid-base regulation, and excretion of nitrogenous waste. Physiol. Rev. 2005; 85:97–177.
156. Wegner NC, Farrell AP. Plasticity in gill morphology and function. In: Alderman SL, Gillis TE, editors. Encyclopedia of fish physiology, 2nd edition. Academic Press, Oxford, 762–779, 2024.
157. Noffke N et al.. Microbially induced sedimentally structures recording an ancient ecosystem in the ca. 3.48 billion-year-old dresser formation, Pilbara, Western Australia. Astrobiology 2013; 13:1103–1124.
158. Ohtomo Y. et al. Evidence for biogenic graphite in early Archaean Isua metasedimentary rocks. Nature Geoscience 2014; 7:25–28.

 doi:10.20944/preprints202512.1208.v1

159. Fish FE. Biomimetics: Determining engineering opportunities from nature. In: Martín-Palma RJ, Lakhtakia A, editors. Biomimetics and bioinspiration. Proc. of SPIE 2017; 7401:740109, 2017.
160. Williams H. Biomimicry in bioengineering: learning from nature to engineer better solutions. Bio. Eng. Bio. Electron. 2024; 6:03
161. Valenzuela C. Nature's solutions: biomimetics and sustainable technology. J. Biomed. Syst.Emerg. Technol. 2024; 11:02.
162. Yue Y (ed.). Proceedings of the 2024 International Conference on Mechanics, Electronics Engineering and Automation (ICMEEA 2024). AER 240. https://doi.org/10.2991/978-94-6463-518-8_61
163. Kennedy EM, Marting TA. Biomimicry: streamlining the front end of innovation for environmentally sustainable products: biomimicry can be a powerful design tool to support sustainability-driven product development in the front end of innovation. RTM 2016; 59:40-48.
164. Kantaros A. et al. Biomimetic additive manufacturing: engineering complexity inspired bynature's simplicity. Biomimetics 2025; 10:453.
165. West BJ. Physiology in fractal dimensions: error tolerance. Ann. Biomed. Engineer. 1090; 18: 135–149.
166. Zueva MV. Fractality of sensations and the brain health: the theory linking neurodegenerative disorder with distortion of spatial and temporal scale-invariance and fractal complexity of the visible world. Front. Aging Neurosci. 2015, 7:135.
167. Torres-Rico M et al. Fractal dimension reveals cellular morphological changes as early biomarkers in neurodegenerative diseases: a narrative review. NeuroMarkers 2025; 2:100108.
168. Tanabe N et al. Fractal analysis of lung structure in chronic obstructive pulmonary disease. Front. Physiol. 2020; 11:603197.
169. John AM et al. The utility of fractal analysis in clinical neuroscience. Rev. Neurosci. 2015; 26:633-645.
170. Uahabi KL, Atounti M. Applications of fractals in medicine. Annals of the University of Craiova, Mathematics and Computer Science Series 2015; 42:167174.
171. Pirri C et al.. The value of fractal analysis in ultrasound imaging: exploring intricate patterns. Appl. Sci. 2024; 14:9750.
172. Marusina MY et al.. MRI image processing based on fractal analysis. Asian Pac. J. Cancer Prev. 2017; 18:51-55.
173. Ruiz de Miras J et al.. Fractal dimension analysis of resting state functional networks in schizophrenia from EEG signals. Front. Hum. Neurosci. 2023; 17:1236832.
174. Albertovich TD, Rusanova IA. The fractal analysis of the images and signals in medical diagnostics: fractal analysis - applications in health sciences and social sciences. InTech. doi:10.5772/intechopen.68167.
175. Paun MA et al.. Fractal analysis in the quantification of medical imaging associated with multiple sclerosis pathology. Front. Biosci. 2022; 27:66.
176. Mahapatra K, Selvakumar R. Fractal dimension and entropy analysis of medical images for KNN-based disease classification. Baghdad Sci. J. 2025; 22: 27.
177. Yoder KJ et al.. Fractal dimension distributions of resting-state electroencephalography(EEG) improve detection of dementia and Alzheimer's disease compared to traditional fractal analysis. Clin. Transl. Neurosci. 2024; 8:27.
178. Bayrak EA, Kirci P. Fractal analysis usage areas in healthcare. In: Zgurovsky M, Pankratova N, editors. System analysis and intelligent computing. SAIC 2020. Studies in Computational Intelligence, vol. 1022. Cham (Switzerland): Springer; 2022.
179. Ziukelis ET et al. Fractal dimension of the brain in neurodegenerative disease and dementia: a systematic review. Ageing Res. Rev. 2022; 79:101651.
180. Li P et al. Interaction between the progression of Alzheimer's disease and fractal degradation. Neurobiol. Aging 2019; 83:21-30.